

Support for a new therapeutic approach of using a low-dose FGFR tyrosine kinase inhibitor (infigratinib) for achondroplasia

Benoit Demuyck,¹ Justine Filpo,¹ Gary Li,² Carl Dambkowski,² Laurence Legeai-Mallet¹

¹INSERM U1163, Imagine Institute, Paris University, Paris, France; ²QED Therapeutics, Inc., San Francisco, California, USA

#5341

Introduction

Fibroblast Growth Factor Receptor 3 (FGFR3) plays a crucial role in the process of endochondral ossification as shown by *FGFR3* gain-of-function mutations that result in common forms of short-stature skeletal dysplasia, such as achondroplasia (ACH).

ACH is the most common cause of rhizomelic dwarfism, an autosomal dominant disorder with an incidence between 1 in 10,000 and 1 in 20,000 live births worldwide.¹

In >95% of cases, ACH is caused by an arginine-to-glycine substitution at residue 380 (p.Gly380Arg) in the *FGFR3* gene; this is an autosomal dominant gain-of-function mutation that demonstrates 100% penetrance and is *de novo* in 80% of cases.²

The ACH phenotypes include rhizomelia (shortening of the limbs with proximal segments affected disproportionately), large head with frontal bossing, mid-face hypoplasia, and relatively normal trunk, with excessive lumbar lordosis.²

Even though they are rare, serious complications are associated with ACH, including cervical spinal cord compression due to a narrowed foramen magnum, lumbar nerve root and/or cord compression due to spinal stenosis, and severe lower extremity vasculature deformity.³

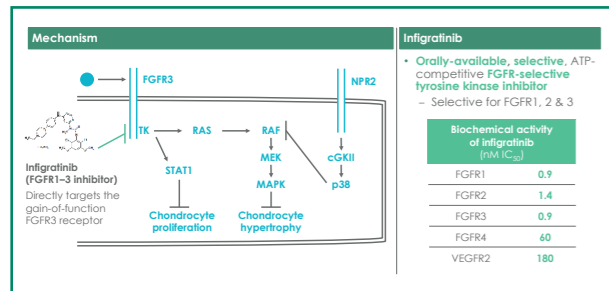
Current management of ACH focuses on the prevention and treatment of its complications as there is no approved therapy that targets the pathophysiology of the condition.

Various therapeutic strategies have been considered, the most advanced being an analog of C-type Natriuretic Peptide (CNP, vosoritide), which is given as a daily subcutaneous injection and acts by antagonizing the MAP kinase pathway. However, both STAT1 and MAPK signaling impact the achondroplasia phenotype.

In this study, we evaluated a therapeutic strategy that targets all pathways downstream of FGFR3.

We hypothesized that a very low dose of the oral selective FGFR1-3 tyrosine kinase inhibitor (TKI) infigratinib (BGJ398) would improve defective bone elongation and have greater potency at lower concentrations in an ACH cell line than a CNP analog (e.g., vosoritide).

Figure 1. Infigratinib directly targets the underlying cause of achondroplasia, FGFR3 overactivity^{2,4}



Objectives and methods

We hypothesized that infigratinib would have greater potency at lower concentrations in an ACH cell line than a CNP analog (e.g., vosoritide) given its effects on multiple pathways downstream of FGFR3. We also hypothesized that a very low dose of infigratinib would be able to improve defective bone elongation in a dose-dependent manner.

The objective of the current studies was to assess *in-vitro* potency of infigratinib and vosoritide in a human chondrocyte line expressing a heterozygous Y373C *FGFR3* mutation and assess *in vivo* the effects of multiple doses of infigratinib on the endochondral process in *Fgfr^{387C/+}* mice using X-rays and macroscopic, histology, and immunohistology analyses.

In-vitro study design

TAN 4-18-chondrocytes, a human chondrocyte line expressing a heterozygous Y373C *FGFR3* mutation, were incubated with increasing concentrations of infigratinib and vosoritide and the total and phospho-ERK1/2 levels were measured by western blot analysis.

Mouse model and drug treatment

The ACH *Fgfr^{387C/+}* mouse model has been described previously.^{5,6}

Phosphate salt (BGJ398-AZA) of infigratinib was used. Infigratinib phosphate was formulated as a suspension for subcutaneous administration in DMSO (1 ml : 2 mg). Infigratinib was given via subcutaneous administration due to the size and age of the mice, which makes oral gavage impractical.

Fgfr^{387C/+} mice were treated from Day 1 (Day 0 = birth) to Day 15 with infigratinib subcutaneously once daily (daily dose of 0.2 mg/kg or 0.5 mg/kg) or every 3 days (intermittent dosing of 1 mg/kg every 3 days). Animals were sacrificed on Day 16. Results were compared with those obtained from mutant mice receiving vehicle.

In-vivo observations

Clinical observations for severity of effect were performed twice a week (hind limb movement, posture, tail, paws), including assessment for survival. Detailed observations were performed at the time of scoring.

X-ray assessments

Lateral X-ray images were taken of all animals by Faxitron MX20 Cabinet X-ray system (Lincolnshire, IL, USA) following terminal sacrifice. Animals were placed on their right side, with the left hind leg more forward than the right, to allow both hind legs to be visible on the X-ray.

Bone length measurement

Bone length was measured using a caliper (WVR1819-0013, VWR, USA) at necropsy.

FGF23 level assessment

FGF23 levels in plasma collected at the end of *in-vivo* studies were determined by ELISA (No. CY-4000) manufactured by Kainos Laboratories.

Phosphorus assessment

Phosphorus levels in plasma collected at the end of *in-vivo* studies were determined by Phosphate Assay kit (Abcam, ab65622).

Statistical analysis

Differences between experimental groups were assessed using ANOVA with Tukey's post-hoc test or Mann-Whitney U-test. The significance threshold was set at $p < 0.05$.

Statistical analyses were performed using GraphPad PRISM (v5.03).

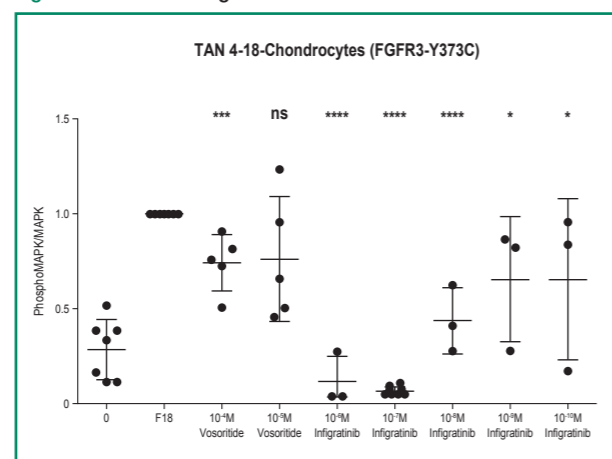
Results

In-vitro results

We observed that in the FGF18-conditioned TAN 4-18-chondrocytes concentrations of 10^{-6} M to 10^{-10} M infigratinib led to statistically significant inhibition of ERK1/2 phosphorylation ($p < 0.05$) compared to untreated cells.

We also observed that vosoritide treatment led to statistically significant inhibition of ERK1/2 phosphorylation at a concentration of 10^{-4} M ($p < 0.05$), but not at 10^{-6} M (not significant) compared with untreated cells.

Figure 2. In-vitro findings



In-vivo efficacy

We observed a statistically significant improvement vs vehicle-treated *Fgfr^{387C/+}* mice in the upper (humerus +7.3%, $p < 0.01$; ulna +11.1%, $p < 0.001$; radius +14.2%, $p < 0.001$) and lower (femur +10.4%, $p < 0.01$; tibia +16.8%, $p < 0.001$) limbs with infigratinib at a dose of 0.5 mg/kg, as well as improvement in the foramen magnum (FM length +11.9%, $p < 0.001$).

The effect of infigratinib on bone elongation was lower at 0.2 mg/kg (Figure 3), indicating a dose-response relationship.

To test whether daily treatment was needed, we performed intermittent injections of infigratinib (1 mg/kg, every 3 days):

As shown in Figure 3, the gain of growth vs vehicle-treated mice was significant for all long bones (humerus +5.0%, $p < 0.001$; ulna +5.6%, $p < 0.001$; radius +4.3%, $p < 0.001$; femur +8.7%, $p < 0.001$; tibia +6.4%, $p < 0.001$) and the foramen magnum was increased (FM length +6.3%, $p < 0.01$).

In addition to the gain of growth, we observed a modification of the growth plate structure, displaying a better organization of the hypertrophic zone, among other improvements (Figures 4 & 5).

Figure 3. Overall findings by dose

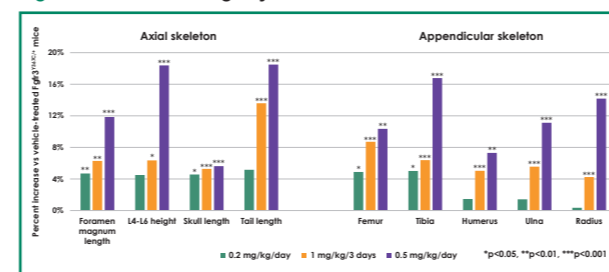
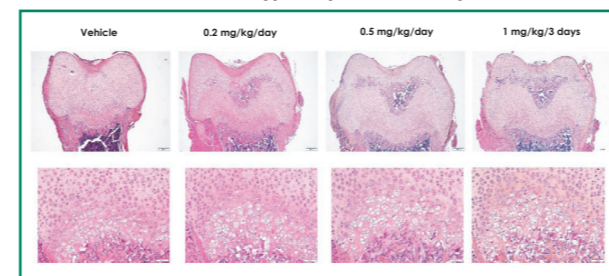


Figure 4. Infigratinib promotes the formation of the ossification center and the number of hypertrophic chondrocytes



The secondary ossification center is larger in infigratinib-treated mice vs control mice. Histological samples demonstrate efficient penetration of the growth plate by infigratinib.

Figure 5. Infigratinib leads to improvement of chondrocyte differentiation in proximal and distal femurs

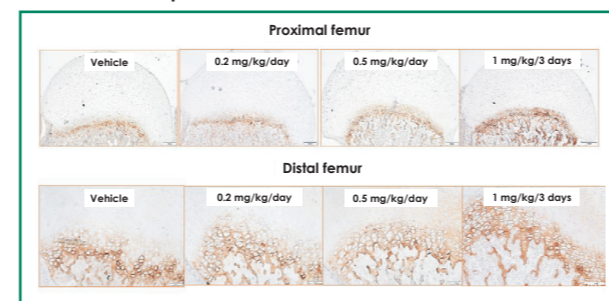
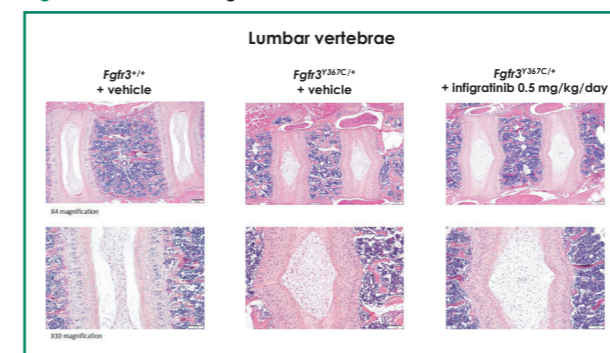


Figure 6. Effects of infigratinib treatment on the intervertebral disc

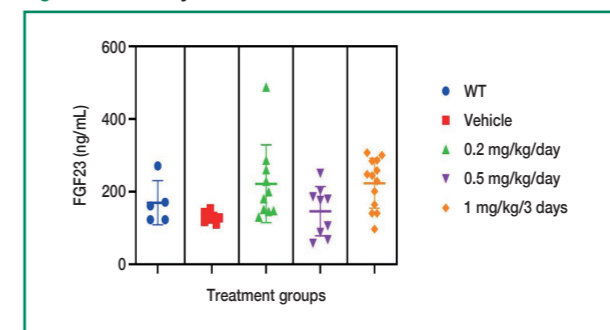


Treatment with infigratinib modified the morphology of the nucleus pulposus and annulus fibrosus.

FGF23 levels in plasma

FGF23 levels by ELISA are shown in Figure 7. No statistically significant differences in FGF23 were observed in infigratinib-treated *Fgfr^{387C/+}* mice vs untreated wild-type mice ($p > 0.05$).

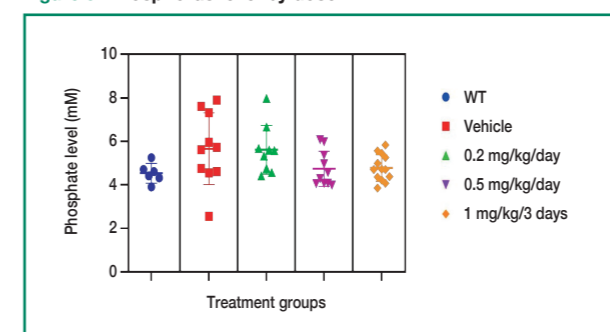
Figure 7. FGF23 by dose



Phosphorus levels in plasma

Phosphorus levels are shown in Figure 8. No statistically significant differences in phosphorus levels were observed in infigratinib-treated *Fgfr^{387C/+}* mice vs untreated *Fgfr^{387C/+}* or wild-type mice ($p > 0.05$).

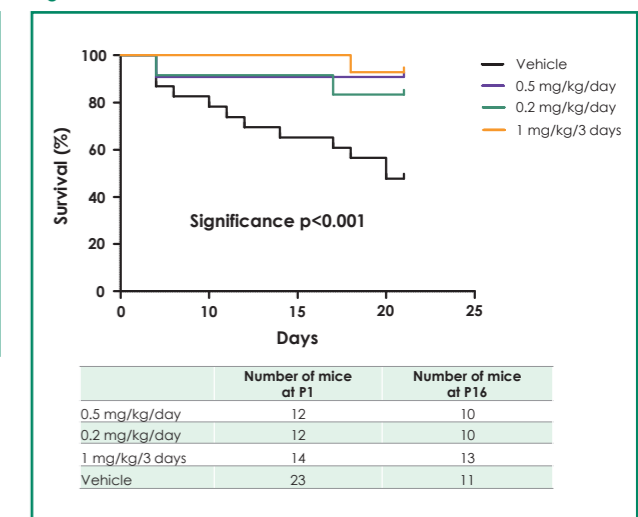
Figure 8. Phosphorus level by dose



Survival

Survival of *Fgfr^{387C/+}* mice treated with infigratinib was improved after 15 days vs vehicle-treated mice ($p < 0.001$ at all doses vs vehicle).

Figure 9. Survival data



Discussion

In-vitro data demonstrate that infigratinib has superior activity over a CNP analog, suggesting that inhibition of multiple key pathways downstream of FGFR3 controlling either proliferation and differentiation of the chondrocytes leads to better efficacy compared with MAPK inhibition alone.

In-vivo data demonstrate that low, as well as intermittent, doses of infigratinib promote growth in this ACH mouse model:

Low-dose infigratinib treatment of *Fgfr^{387C/+}* mice over 15 days improved the endochondral ossification processes in an ACH mouse model.

Skeletal changes were observed in a dose-dependent manner, based on total dose given over the treatment period.

At the doses of infigratinib examined in these experiments, FGF23 and phosphate levels did differ from wild-type mice, demonstrating that low-dose infigratinib can affect dysfunctional FGFR3 signaling in an ACH mouse model while having no measurable impact on downstream changes in FGFR1/4, which is an important signaling pathway regulating phosphate reabsorption in renal cells.

No apparent toxicity of infigratinib was observed in treatment mice or seen via laboratory measures performed; on the contrary, treatment of *Fgfr^{387C/+}* mice with infigratinib improved survival compared with untreated mice.

Conclusion: these results suggest that, at low doses, TKI therapy with infigratinib has the potential to be a valuable and relevant therapeutic option for children with ACH. These findings support the continued development of infigratinib as a treatment for ACH, with clinical studies planned to begin this year.

References

- Horton WA, et al. *Lancet* 2007;370:162–72.
- Ornitz DM & Legeai-Mallet L. *Developmental Dynamics* 2017;246:291–309.
- Hoover-Fong J, et al. *Am J Med Genet A* 2017;173:1226–30.
- Guagnano et al. *JMC* 2011.
- Lorget F, et al. *Am J Hum Genet* 2012;91:1108–14.
- Pannier S, et al. *Biochim Biophys Acta* 2009;1792:140–7.